# COMPARISON OF MODIS AND MISR-DERIVED SURFACE ALBEDO WITH IN SITU MEASUREMENTS IN GREENLAND

*J. Stroeve and A. Nolin*

*National Snow and Ice Data Center (NSIDC), Cooperative Institute for Research in Environmental Sciences (CIRES), University of Colorado, Campus Box 449, Boulder, CO 80309-0449, Tel. 303-492-3584, Fax. 303-492-2468, email: stroeve@kodiak.colorado.edu*

## ABSTRACT

Accurate estimation of snow albedo is essential for monitoring the state of the cryosphere. The high albedo of snow-covered surfaces allows little energy to be absorbed by the snowpack. However, as snow ages and/or begins to melt the albedo decreases and more energy is absorbed by the snowpack. This paper examines the retrieval of snow albedo from the MISR and MODIS instruments over the Greenland ice sheet. Two different methods are used to compute the albedo. The first method uses spectral information from MISR and MODIS. The second method uses angular information from MISR to develop a statistical relationship between *in situ* albedo and the red channel reflectance at all nine MISR viewing angles. Good agreement with *in situ* measurements is found using either method, although problems with instrument calibration, snow BRDF models and narrow-to-broadband albedo relationships can cause the albedo error to still be large with the first method. With a few exceptions, the satellite-derived surface albedo is within about 6% of that measured at the stations.

## INTRODUCTION

The surface albedo is an important climate parameter, as it influences the amount of solar radiation absorbed by the surface. Satellite remote sensing offers a means for measuring and monitoring the surface albedo of snow-covered surfaces. Several studies have attempted to estimate the albedo over snow in the polar regions using visible and near infrared (NIR) data from sensors such as the NOAA Advanced Very High Resolution Radiometer (AVHRR) [e.g. (1)-(2)]. Snow albedo is also one of the standard products to be generated in the near future from data acquired by the Moderate Resolution Imaging Spectroradiometer (MODIS) instrument flown on the Terra satellite (3). Snow albedo from instruments such as AVHRR and MODIS rely on using variations in spectral reflectance to derive the albedo. With the Multiangle Imaging SpectroRadiometer (MISR), also flown on Terra, the possibility exists to use the angular signatures in addition to spectral signatures for high-resolution snow albedo retrievals.

This study evaluates snow surface albedo retrievals from MISR and MODIS through comparisons with ground-based surface albedo measurements obtained in Greenland. Two different techniques will be examined for deriving the surface albedo. One using angular information from MISR and the other based on spectral information from both MISR and MODIS. Data from automatic weather stations (AWS) during 2000 and 2001, in addition to other in situ data collected during summer 2000 provide the ground-based measurements with which to compare coincident clear-sky satellite albedo retrievals.

## DATA SETS

### *A. Greenland In Situ Data*

The *in situ* albedos come from five AWS that are part of the Greenland Climate Network (GC-Net) (4).

Swiss Camp - located at the equilibrium line altitude on the western side of the ice sheet [69°59N, 49°27W; 1150 m a.s.l.].

JAR - situated in the ablation region near Swiss Camp [69.50°N, 49.69°W; 962 m a.s.l.].

Summit - located at the highest point of the ice sheet [72.58°N, 38.50°W; 3150 m a.s.l.].

TUNU-N - located in a relatively low accumulation region of the ice sheet in the northeast [78.02°N, 33.99°W; 2113 m a.s.l.].

Humboldt - situated in a relatively high accumulation region of the ice sheet in the northwest [78.53°N/56.83°W; 1995 m a.s.l.].

All the AWS employ LI-COR 200SZ photoelectric diodes to measure incoming and reflected solar radiation from 0.4-1.1 μm. This spectral range does not cover the entire solar spectrum, such as what is typically measured by an albedometer or by a pyranometer [e.g. 0.3-2.5 μm]. Relative calibration of the LI-CORs versus pyranometers at the Swiss Camp in Greenland reveals that the LI-COR-derived albedo is about 4% greater than that measured by pyranometers (5). However, this bias may not be applicable to other stations since the difference in measured albedo between the two instruments will depend on both atmospheric and surface conditions. For example, based on model simulations of snow albedo, the difference between LI-COR and Eppley Precision Spectral Pyranometer (PSP) albedo for fine-grained snow [e.g. grain size of 50 μm] is 5.2%, whereas for a snow grain size of 1000 μm, the difference is 13.2%. Thus, we stress here that caution is needed when making comparisons between the broadband albedo being derived from satellite and the LI-COR-measured surface albedo since the measurements correspond to different spectral ranges.

From 18 May to 2 June 2000, albedo and atmospheric data were collected at Swiss Camp. During the course of the field experiment, the broadband albedo [0.3–2.5μm] was measured using a pair of Eppley PSP. The instruments were calibrated before and during the course of the field experiment and provide estimates of surface broadband albedo averaged over five minute intervals. In addition to the albedo measurements, atmospheric characterization of aerosols, ozone and water vapor were performed using a spectrally filtered, solar-pointing radiometer supplied by the Jet Propulsion Laboratory (JPL). During periods of calibration of the instrument and at times consistent with the Terra satellite overpass, measurements were made every ten minutes. Otherwise, measurements were made once every hour. Aerosol optical depth was computed using the Langley plot method following the methodology described in (6). Measured aerosol optical depths at 520 nm ranged from 0.04 to 0.09.

Because of its narrow orbital swath, no concurrent MISR data were available during clear-sky periods between 18 May and June 2000. Therefore, only the MODIS-retrieved surface albedo will be compared with the pyranometer-measured surface albedo at the Swiss Camp during this time period. All other comparisons will be made with LI-COR measured albedo.

### *B. Modis*

The MODIS instrument is onboard the NASA Earth Observing System (EOS) Terra satellite which was launched 18 December 1999. The MODIS data used for this comparison study come from the Level1B data set. This data set contains calibrated and geolocated radiances for 36 bands. The spatial resolutions of the different spectral bands are as follows: bands 1 and 2 at 250m, bands 3-7 at

500m, and bands 8-36 at 1000m spatial resolution. The top-of-the-atmosphere (TOA) Bidirectional Reflectance Factor (BRF) can be determined for the solar reflective bands [1-19, 26] through knowledge of the solar irradiance which is determined from the MODIS diffuser data and from the target illumination geometry. The Level 1B visible and near-infrared (NIR) radiances were converted to TOA BRF and gridded to the 1.25-km Equal-Area Scalable Earth-Grid [EASE-Grid, (7)]. The MODIS channels used in this study and their respective wavelengths are: ch1[0.650μm], ch2[0.847μm], ch3[0.470μm], ch4[0.550μm] and ch5[1.247μm]. Band 6 has been found to not be reliable [D. Hall, pers. comm.] and band 7 [at 2.130μm] does contribute much to the albedo over snow. Examination of the MODIS radiance data indicates that the other visible channels become saturated over Greenland [e.g. channels 8-15]. For each station, a 10 by 10 sub-region is extracted around the camp. Fourteen clear-sky MODIS images were acquired during summer 2000.

### *C. MISR*

The Terra MISR instrument uses nine discrete cameras pointed at fixed angles, one looking straight down [nadir], and four viewing angles in both the forward (f) and aftward (a) directions along the spacecraft ground track. The four angles on either side of nadir are: 26.1, 45.6, 60.0 and 70.5 degrees, referred to as the A, B, C and D cameras, respectively. The nadir camera is called the An camera. For this work, the MISR L1B2T [terrain-registered] TOA scaled radiance data are used. The L1B2 data are in a Space Oblique Mercator (SOM) grid, such that each orbital path is gridded into 180 blocks. The red channel data are at 275-m resolution for all cameras, as are the blue, green, red and near-infrared channels of the nadir camera. All other channels, in the instrument's Global Mode, are at 1.1-km resolution. Here we only use the 275-m resolution data. For each region of interest, the following cameras and channels are extracted for a 50 by 50 pixel sub-region centered on each station: Df-red, Cf-red, Bf-red, Af-red, An-blue, An-green, An-red, An-NIR, Aa-red, Ba-red, Ca-red, Da-red [blue=0.446μm, green=0.558μm, red=0.672μm, NIR=0.867μm]. The subset data are converted from TOA scaled radiances to TOA BRF using TOA solar irradiance and solar zenith angle data supplied with the MISR imagery. A total of 29 clear-sky MISR images over Greenland from May 2000 to August 31 2001 were collected for this study.

## CLEAR-SKY ALBEDO METHODOLOGY

### *A. Snow Surface Albedo from Spectral Information*

The methodology used to derive the surface albedo using the satellite spectral data is similar to (1) where the following three steps are performed in sequential order:

1) Correction for atmospheric effects.
2) Correction for anisotropic reflection at the surface.
3) Calculation of the spectrally integrated albedo.

#### 1. Atmospheric Correction

Atmospheric correction for MODIS and MISR is performed using the 6S radiative transfer (RT) model (8). To account for the polar environment, additions were made to the RT model which included the following: addition of standard Arctic summer and winter atmospheric profiles; spectral albedo of new and old snow; and snow Bidirectional Reflectance Distribution Functions (BRDF) for MODIS and MISR. For comparisons with station data, 6S is run only for the center pixel for each region extracted around the station location. Atmospheric parameters obtained from running 6S for the center pixel are then used to derive the surface albedo for each pixel in the sub-regions assuming that atmospheric conditions and sun-sensor angles remain constant over the sub-region. At Swiss Camp and JAR, during the May/June 2000 field campaign, aerosol and ozone optical

depths and atmospheric water vapor amounts as obtained by Sunphotometer measurements at the Swiss Camp are used as input. At the other stations, aerosol optical depths are assumed to be 0.02 for Summit, 0.04 for Humboldt, and 0.03 for TUNU-N. Ozone and water vapor are taken from a standard arctic summer atmospheric profile assuming surface elevations according to each site. During other time periods when measurements of atmospheric optical depths are not available, the aerosol optical depth is assumed to be 0.08 at JAR and 0.06 at Swiss camp. The atmospherically-corrected satellite measurement is referred to as the hemispherical directional reflectance factor (HDRF).

2. Anisotropic Correction

To correct for the angular anisotropy of the snow surface, the HDRF of the snow surface is simulated using a radiative transfer model. The Mie scattering parameters for ice grains of a specified radius are input to the DIScrete Ordinates Radiative Transfer model [DISORT; (9)]. DISORT computes the surface HDRF and albedo for specified viewing and solar geometries, and proportions of diffuse and direct illumination. The ratio of the albedo to the HDRF becomes the conversion factor by which the satellite-derived HDRF is then multiplied to obtain the spectral surface albedo for each satellite channel.

For each image to be processed, the direct and diffuse components are obtained using the 6S atmospheric radiative transfer model. The direct and diffuse components for each satellite channel and specific sun-sensor angular geometry is then input into DISORT to derive the conversion factors for each region of interest. In running the DISORT model, a snow grain size of 250 μm was assumed when measurements were otherwise not available. For snow conditions during July and August near the Swiss camp, it is likely that much larger grain sizes occur because of snow melt.

3. Narrow-to-Broadband Albedo Conversion

In general, a linear relationship between the narrowband and the broadband albedo is used [e.g. (1) and (10) among many others] so that the broadband albedo is derived from the following type of equation:

$$broadband = a_o + b_1 ch_1 + b_2 ch_2 + ... + b_n ch_n + \varepsilon \qquad (1)$$

where $a_o$, $b_1$, $b_2 \ldots b_n$ are regression coefficients derived from multiple linear regression on the satellite channels ($ch_i$) versus the broadband albedo. The regression coefficients in (1) are not only dependent on surface conditions; they are also dependent upon atmospheric conditions. The downward irradiance distribution at the bottom of the atmosphere is the weighting function for converting the narrowband albedos to broadband albedos. Thus, a relationship developed under a specific surface/atmospheric condition may not be valid under different conditions from which the relationship was developed. This is one reason why published narrow-to-broadband relationships differ widely. Another reason why narrow-to-broadband relationships differ widely is because the independent variables [$ch_1 \ldots ch_n$] are highly interdependent. In this situation, the sampling distributions of the estimated regression coefficients can become very broad, with the consequence that a forecasting equation may perform badly when implemented on future data independent of the training sample. For this study we chose to test the models given in (10) which results in a broadband albedo (e.g. from 0.3 – 2.5 μm).

*B. Snow Surface Albedo from MISR Angular Information*

The variation of surface reflectance with viewing and illumination angle is another source of information contained within the MISR data besides the spectral content. Thus, it may be possible to use angular information from MISR to directly compute the surface albedo. We start with the red channel multiangle observations that have been atmospherically corrected [e.g. the HDRF] using the atmospheric correction method discussed previously, and attempt to derive a statistical model relating the multiangle measurement to the surface albedo. In selecting variables for input into the linear re-

gression model, primary consideration is given to those variables most directly related to the surface albedo.

Generally, the relationship between the surface albedo and the shape of the HDRF [e.g. see Figure 1] depends on both the solar zenith angle and the snow grain size. However, grain size is typically not known, and therefore, is not used as a predictor variable. Here we use a forward-screening linear regression model to select the predictor variables. The first parameter used is the area under the red spectral channel HDRF curve in the principal plane for each station analysed. The model then searches through the remaining variables [e.g. solar zenith angle, spectral reflectance in red at all viewing angles, nadir spectral reflectance in blue, green, red and NIR] and selects the ones providing the best improvement in the squared correlation. If the improved explained variance exceeds a threshold of 5%, the variable is included in the multiple linear regression. Using this technique, three predictor variables are selected: integral of red HDRF over all viewing angles [both forward and aftward directions], cosine of the solar zenith angle, and the nadir NIR HDRF.

Since there are not enough clear-sky MISR images to construct a regression model [we currently only have 29 MISR clear-sky images over Greenland] and then use that model on independent MISR data to predict the albedo, a 'Bootstrap' regression approach is used. In this approach a regression model is derived using all the stations except the one to be predicted. This is done for each station in turn, resulting in 29 different regression models. Next, the surface albedo is predicted at each station location using the regression model based on data from all the other stations. Note that in deriving the regression models, regression is performed with the LI-COR-measured surface albedo, and thus the albedo predicted using this method corresponds to the spectral range of the LI-COR measurement [0.4-1.1μm].

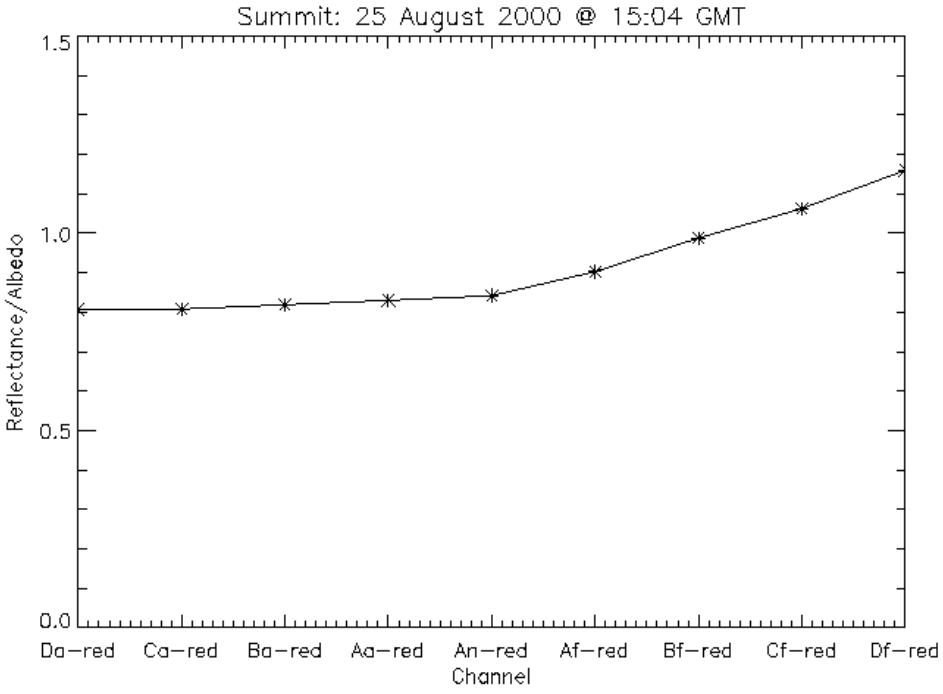


*Figure 1: Example of the surface HDRF in both the forward (f-cameras) and aftward (a-cameras) directions at each MISR viewing angle. The area under this curve is used as a predictor variable in the multiangle albedo retrieval method. Note that the shape of this curve depends on the snow grain size and on the solar zenith angle.*

## RESULTS

Figure 2 (a) - (e) compares the MISR albedo estimates with the ground-based measurements at JAR, Swiss Camp, Summit, Humboldt and TUNU-N. Shown in (2) is the albedo for each acquisition date determined by averaging 10 pixels around the station using both methods. Notice that in

most cases the albedo retrieved using the spectral method is less than the LI-COR measured albedo. This is expected because the albedos represent different spectral regions.

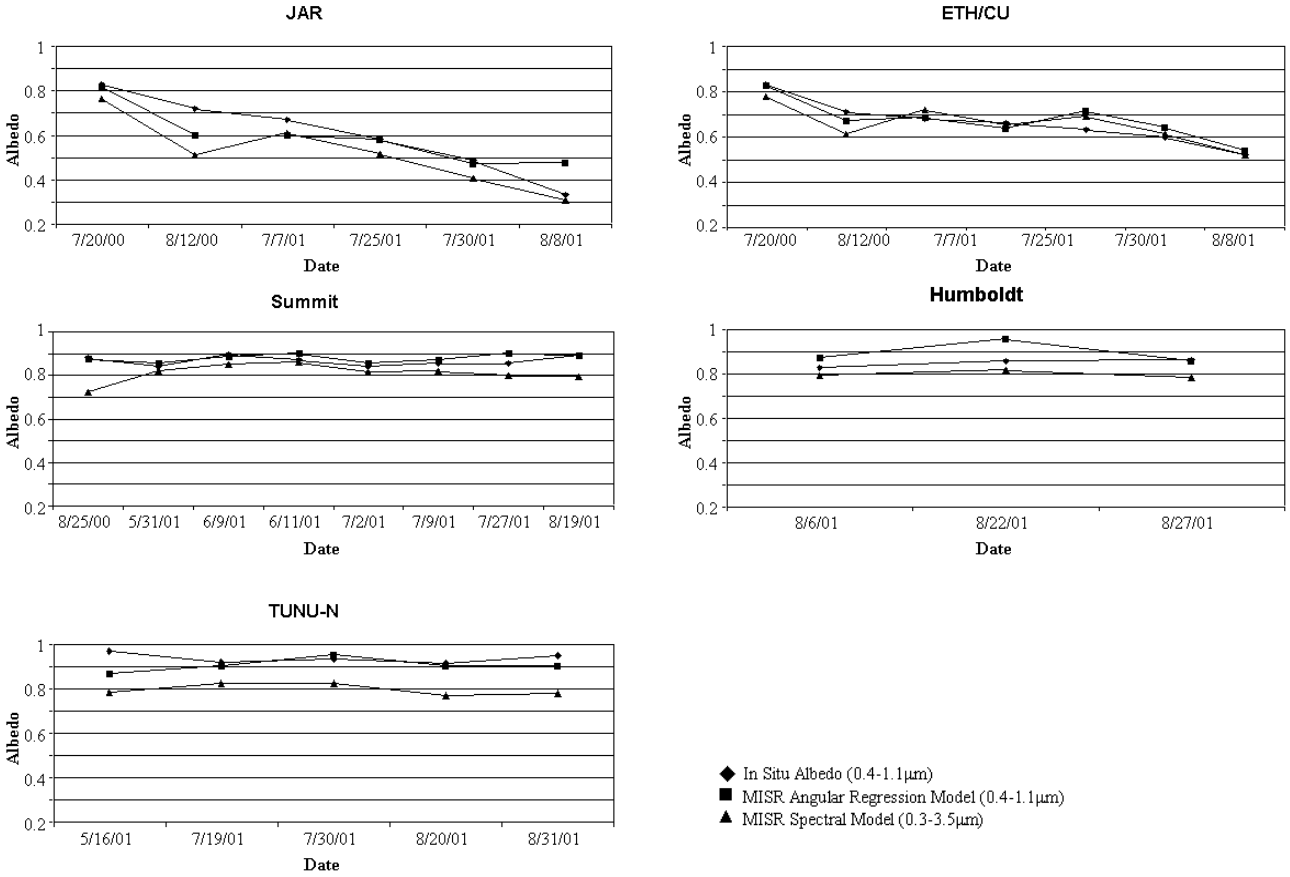


*Figure 2: Comparison of surface albedo at JAR, Swiss Camp, Summit, Humboldt and TUNU-N as a function of date. The solid line shows the in situ albedo [0.4-1.1μm], the dotted line is the albedo derived from the statistical relationship based on the MISR angular data, and the dashed line is the albedo derived from a linear combination of the MISR spectral channels.*

In general, agreement between MISR-derived and *in situ* albedo is good at all stations using either method. Some notable exceptions occur at TUNU-N using the spectral albedo retrieval method, at Humboldt using the statistical multiangle retrieval method on 8/22/01 and at JAR on 8/12/00 using either method. One reason for the discrepancy at JAR on 8/12/00 could be because the surface is quite inhomogeneous around the station. Summer melt is active during July and August in this region, and several melt ponds are evident near the station. The larger footprint size of the satellite measurement could pick up some of the neighbouring melt ponds resulting in lower albedos than measured at the station. Melting at Swiss Camp during summer could also explain why the *in situ* albedo is lower than the satellite- derived values. It is entirely possible, that there is localized melting at the station that is not represented in the larger footprint size of the satellite measurement, causing the *in situ* albedo to be less than the satellite-derived albedo. However, even though the inhomogeneous surface near JAR and Swiss Camp during summer makes it difficult to compare the *in situ* and satellite-retrieved albedo, the MISR-derived albedo is qualitatively correct, showing a decrease in albedo as the snow melts.

Conversely, much less variability in albedo is found at the higher elevation sites, which do not experience any ablation. For example, at Summit the mean difference between satellite and *in situ* albedo is 1.5% using the multiangle retrieval method and 6.4% using the spectral method [given the positive bias of the LI-COR measurement of a few percent the agreement it good]. At TUNU-N the albedo obtained using the spectral albedo method is approximately 12.5% lower than measured at the station. We expect the LI-COR albedo to be biased slightly high [~ 6% for small grain sizes]

compared with the satellite estimate using the spectral method. However, at this station the *in situ* albedo values are all greater than 0.9. The surface albedo could be in excess of 0.9 for very new snow with small grain sizes, but values near 0.97 are too high. The primary source of error in the *in situ* albedo is instrument level [J. Box, pers. comm.]. The instruments are re-leveled every 1-2 years to minimize this error, but biases due to instrument level likely remain.

Figure 3(a)-(c) show MODIS-derived and *in situ* measured albedo at JAR, Swiss camp and Summit as a function of date and time. Two different MODIS-retrieved surface albedos are shown. One assuming Lambertian conditions [dashed line] and one using the conversion factors to correct for the snow anisotropy [dotted line].

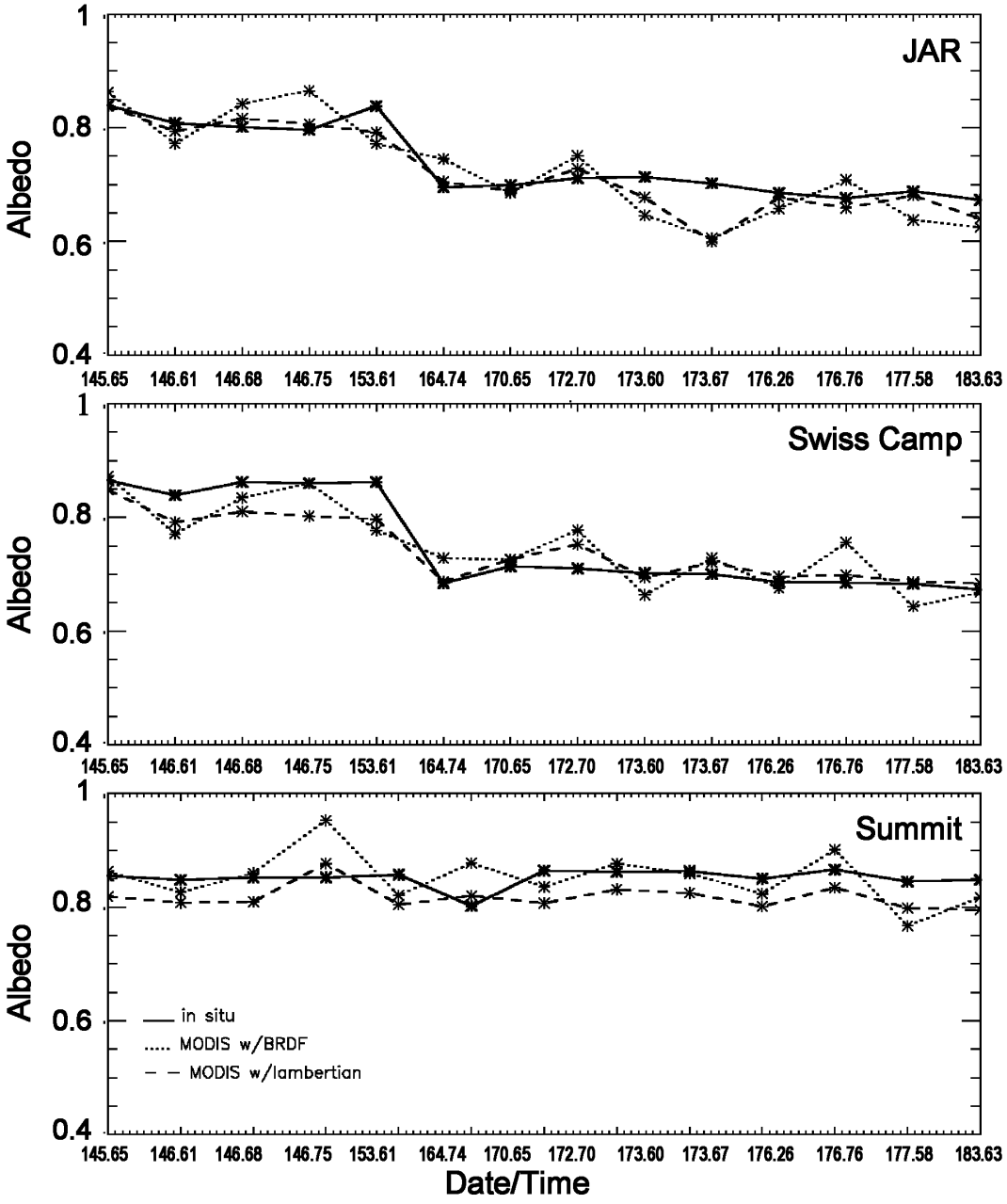


*Figure 3: Comparison of surface albedo at JAR, Swiss Camp and Summit as a function of date and time. Solid line shows the in situ albedo [from 0.4-1.1µm, except for days 145-153 at Swiss Camp when the albedo is from 0.3-2.5 µm]. The dotted line is the albedo computed using anisotropic conversion factors and the dashed line is the albedo derived assuming the surface is a perfect Lambertian reflector.*

For days 145 to 153 at Swiss Camp, the *in situ* albedo is measured by the PSP. After day 153 the albedo come from the LI-COR measurements. Large variability in the MODIS-derived albedo is seen. Some of the variability appears to be a result of the angular conversion factors inadequately accounting for the variation of the albedo with viewing angle. On days 146 [17:55 GMT], 164 [17:45 GMT] and 176 [18:10 GMT] the satellite viewing zenith angles are all greater than 60 degrees. On these days it appears that the angular model is overcorrecting the surface HDRF. Because of this, the surface albedo derived assuming Lambertian conditions at times performs better than when the angular conversion factors are applied. This problem was avoided when computing albedo from the MISR spectral data because only the nadir view was used. The conversion factors are approximately 1 at nadir.

In general, the satellite-derived albedos follow the trends in the *in situ* measurement. After June 01 2000 [day 153], the surface albedo dropped at the Swiss Camp and at JAR as the snow surface began to melt. This is picked up most prominently in MODIS channel 2 [0.847 μm] and is reflected also in the resulting broadband albedo. Conversely, at Summit the MODIS-derived albedo is nearly constant except on days 146 [17:55 GMT] and 176 [18:10] GMT when the angular model appears to have overcorrected the surface HDRF. Overall mean differences are less than 6%, with the smallest mean differences occurring at the Summit station.

## DISCUSSION AND CONCLUSIONS

The albedo derived from satellite radiances is subject to several possible sources of error, including instrument calibration errors, errors in the atmospheric correction, errors in the anisotropic conversion factors, errors in the narrow-to-broadband albedo conversion and differences between the LI-COR albedo and a 'true' broadband albedo. Additional reasons for the observed differences between the *in situ* and satellite-derived albedo include cloud-contamination, surface roughness effects and spatial inhomogeneity. Some of these errors are minimized using the angular statistical model since the model is developed by directly relating the satellite measurement to the LI-COR measurements. Thus, this method may have some advantages, in particular the ease in which such a model can be implemented. However, at this stage it is not possible to say which method gives overall better results. Validation with more MISR and MODIS imagery is needed to make any conclusive statements about the performance of either method. Both methods however capture the general variability and magnitude of the surface albedo. Future work will involve improving and validating the angular conversion models, narrow-to-broadband albedo models and the MISR angular statistical albedo model.

## REFERENCES

1. Stroeve, J., A. Nolin and K. Steffen, 1997. Comparison of AVHRR-derived and *in situ* surface albedo over the Greenland ice sheet, Remote Sens. Environ., 62:262-276.
2. Knap, W. H. and J. Oerlemans, 1996. The surface albedo of the Greenland ice sheet: satellite-derived and in situ measurements in the Søndre Strømfjord area during the 1991 melt season, J. Glaciol., 42(141):364-374.
3. Klein, A. G. and D. K. Hall, 1999. Snow albedo determination using the NASA MODIS instrument", *Proc. East. Snow Conf.*, 55th Annual Meeting, 2-4 June 1999, Fredericton, New Brunswick, Canada, pp. 77-85.
4. Steffen, K., J. E. Box, and Abdalati, W., 1996. Greenland Climate Network:GC-Net, in CRREL 96-27 Special Report on Glaciers, Ice Sheets and Volcanoes, trib. to M. Meier, Colbeck, S. C. Ed., 98-103.

5. Stroeve, J.C., J.E. Box, C. Fowler, T. Haran, and J. Key, 2001. Intercomparison Between in situ and AVHRR Polar Pathfinder-derived Surface Albedo over Greenland, Remote Sens. Environ., 75(3):360-374.
6. Bruegge, C.J., R.N. Halthore, B. Markham, M. Spanner, and R. Wrigley, 1992. Aerosol optical depth retrievals over the Konza Praire, J. Geophys. Res., 97(D17):18,743-18,758.
7. Armstrong, R.L. and M.J. Brodzik, 1995. Earth-gridded SSM/I data set for cryospheric studies and global change monitoring, in A1 Symposium of COSPAR Scientific Commission A, Hamburg, Germany, July 11-21, 1994. Proceedings: Satellite monitoring of the earth's surface and atmosphere, Nov. 1995, 15-163.
8. Tanre, D., Holben, B.N., and Kaufman, Y.J., 1992. Atmospheric correction algorithm for NOAA-AVHRR products: theory and application, IEEE Trans. Geosci. Remote Sens., 30:231-250.
9. Stamnes, K., S-C. Tsay, W. Wiscombe, and K. Jayaweera, 1988. Numerically stable algorithm for discrete-ordinate-method radiative transfer in multiple scattering and emitting layered media, Applied Optics, 27:2502-2509.
10. Liang, S., 2001. Narrowband to broadband albedo conversions of land surface albedo I - algorithms, Rem. Sens. Environ., 76:213-239.